


# All-trans retinoic acid improves NSD2-mediated RAR $\alpha$ phase separation and efficacy of anti-CD38 CAR T-cell therapy in multiple myeloma

Ziyi Peng,<sup>1</sup> Jingya Wang,<sup>1</sup> Jing Guo,<sup>2</sup> Xin Li,<sup>1</sup> Sheng Wang,<sup>1</sup> Ying Xie,<sup>3</sup> Hongmei Jiang,<sup>1</sup> Yixuan Wang,<sup>1</sup> Mengqi Wang,<sup>1</sup> Meilin Hu,<sup>4</sup> Qian Li,<sup>2</sup> Yafei Wang,<sup>2</sup> Jian-Qing Mi,<sup>5</sup> Zhiqiang Liu <sup>1,2</sup>

**To cite:** Peng Z, Wang J, Guo J, et al. All-trans retinoic acid improves NSD2-mediated RAR $\alpha$  phase separation and efficacy of anti-CD38 CAR T-cell therapy in multiple myeloma. *Journal for ImmunoTherapy of Cancer* 2023;**11**:e006325. doi:10.1136/jitc-2022-006325

► Additional supplemental material is published online only. To view, please visit the journal online (<http://dx.doi.org/10.1136/jitc-2022-006325>).

ZP and JW contributed equally.  
Accepted 17 February 2023



© Author(s) (or their employer(s)) 2023. Re-use permitted under CC BY-NC. No commercial re-use. See rights and permissions. Published by BMJ.

<sup>1</sup>Department of Physiology and Pathophysiology, Tianjin Medical University, Tianjin, China

<sup>2</sup>Cancer Institute and Hospital, Tianjin Medical University, Tianjin, China

<sup>3</sup>Department of Hematology, Tianjin Medical University General Hospital, Tianjin, China

<sup>4</sup>School of Stomatology, Tianjin Medical University, Tianjin, China

<sup>5</sup>School of Medicine, Shanghai Jiao Tong University, Shanghai, China

## Correspondence to

Dr Zhiqiang Liu;  
zhiqiangliu@tmu.edu.cn

Jian-Qing Mi;  
jianqingmi@shsmu.edu.cn

## ABSTRACT

**Background** Immunotherapies targeting CD38 have demonstrated salient efficacy in relapsed/refractory multiple myeloma (MM). However, loss of CD38 antigen and outgrowth of CD38 negative plasma cells have emerged as a major obstacle in clinics. All-trans retinoic acid (ATRA) has been reported to upregulate CD38 expression, but the mechanism and adaptive genetic background remain unexplored.

**Methods** The efficacy of ATRA in upregulating CD38 expression in MM cells is evaluated by flow cytometry. The interaction between NSD2 and the RAR $\alpha$  is analyzed by immunoprecipitation, and the nuclear condensation of RAR $\alpha$  is evaluated under laser confocal microscope. A graft model of MM is established in NOD.*Cg-Prkdc<sup>scid</sup>//2rg<sup>dm1Wjl</sup>/SzJ* mice, and the tumor burden is assessed by in vivo fluorescence imaging.

**Results** We report that ATRA upregulates MM cells CD38 in a non-linear manner, which is t(4;14) translocation dependent, and t(4;14) translocation-induced NSD2 shows positive correlation with ATRA-induced level of, but not with basal level of CD38 expression. Mechanistically, NSD2 interacts with the ATRA receptor, RAR $\alpha$ , and protects it from degradation. Meanwhile, NSD2 enhances the nuclear condensation of RAR $\alpha$  and modifies the histone H3 dimethylation at lysine 36 on CD38 promoter. Knockdown of NSD2 attenuates the sensitization of MM against ATRA induced CD38 upregulation. Translationally, ATRA is prone to augment the efficacy of anti-CD38 CAR T cells in NSD2<sup>high</sup> MM cells in vitro and in vivo.

**Conclusion** This study elucidates a mechanism of ATRA in regulating CD38 expression and expands the clinical potential of ATRA in improving immunotherapies against CD38 in patients with MM. Cite Now

## INTRODUCTION

Multiple myeloma (MM) is a hematological malignancy characterized by the uncontrolled proliferation of clonal plasma cells,<sup>1</sup> accounting for nearly 15% of hematological malignancies.<sup>2</sup> MM remains incurable because the majority of patients eventually relapse or become refractory to the current

## WHAT IS ALREADY KNOWN ON THIS TOPIC

⇒ Immunotherapies targeting CD38 have demonstrated salient efficacy in relapsed/refractory multiple myeloma (MM); all-trans retinoic acid (ATRA) has been proposed to enhance the expression of CD38 antigen.

## WHAT THIS STUDY ADDS

⇒ ATRA enhances the NSD2-mediated nuclear condensation of RAR $\alpha$  and chromatin remodeling on CD38 promoter to upregulate t(4;14) MM cells' CD38 expression in a non-linear manner and, combined with anti-CD38 CAR T-cell therapy, shows significant efficacy in vitro and in vivo.

## HOW THIS STUDY MIGHT AFFECT RESEARCH, PRACTICE OR POLICY

⇒ This study validates the effect of ATRA in enhancing therapeutic efficiency of anti-CD38 CAR T cells in the t(4;14) MM and suggests that combination of anti-CD38 CAR T cells with ATRA is a promising approach to improve tumor cell elimination in patients with t(4;14) MM.

chemotherapies due to genetic alterations within tumor cells and stimuli from bone marrow microenvironment,<sup>3</sup> despite successful application of novel chemicals and current immunotherapies.<sup>4</sup> Frequent IgH translocation is a character of MM and contributes to disease progression and treatment outcomes. For example, translocation involving chromosomal loci 4p16 rendering high expression of NSD2, a histone methyltransferase specific for methylation of histone 3 lysine 36 (H3K36), is a high-risk factor of poor prognosis for patients with MM.<sup>5</sup> However, the roles of NSD2 in regulating sensitivity to chemotherapies, especially to immunotherapies, have not been well illustrated, which demonstrates an unmet requirement for underlying mechanistic studies.

Immunotherapies, including immunomodulatory drugs, anti-CD38 antibody (Ab) daratumumab, the bispecific antibodies and adoptive cell therapy with T cells engineered to express chimeric antigen receptors (CARs), have achieved great clinical successes for managing patients with relapsed or refractory multiple myeloma (RRMM).<sup>6</sup> Indeed, daratumumab has been moved to the frontline regimens for newly diagnosed MM.<sup>7</sup> Nevertheless, clinical studies have indicated that relapse is common across patients who achieve remission after CAR T-cell therapy, indicating the occurrence of immunotherapy resistance.<sup>8</sup> CD38 is highly expressed on MM cells but relatively low on other hematopoietic cells and non-hematopoietic tissues, making it a promising target of CAR T and monoclonal Ab immunotherapies.<sup>9</sup> Low levels of CD38 on a subclone of MM cells, loss of CD38 antigen, and outgrowth of CD38 negative tumor cells have been suggested as main mechanisms of immunotherapy escape. Thus, promoting antigen expression or maintaining antigen stability, using the currently approved agents, holds promise for broadening the immunotherapeutic benefits.

All-trans retinoic acid (ATRA) is a natural oxidative metabolite of vitamin A (retinol) and is a regulator of cell proliferation and differentiation.<sup>10</sup> ATRA has been known as a therapeutic agent for patients with acute promyelocytic leukemia with the PML-RAR $\alpha$  fusion gene in clinics.<sup>11</sup> In mammalian cells, ATRA binds to the retinoid receptors (RARs and RXRs) that consist of RAR $\alpha$ , RAR $\beta$ , and RAR $\gamma$  and RXR $\alpha$ , RXR $\beta$ , and RXR $\gamma$  respectively.<sup>12</sup> The RXR-RAR or RXR-RXR homodimers are ligand-dependent transcription factors.<sup>13 14</sup> After being bound by ligands, RARs bind to retinoic acid response elements and recruit a protein complex, including epigenetic regulators and other transcription factor, to activate gene transcription.<sup>15 16</sup> Notably, ATRA was reported to induce CD38 expression in human tumors including MM,<sup>17–19</sup> thus improving the efficacy of daratumumab<sup>20</sup> and CD38 CAR T-cell therapy.<sup>19</sup> Intriguingly, increasing pieces of evidence have shown that efficacy of ATRA is genetic background dependent, since epigenetic and transcriptional status may correlate with its sensitivity.<sup>21 22</sup> Thus, identification of determinants underlying ATRA sensitivity is a top priority, which could predict clinical benefit of ATRA-based therapies. Actually, MM is a highly heterogeneous disease which highlights the importance of exploring elements governing ATRA sensitivity in MM subtypes.

Recently, protein condensations, such as liquid-liquid phase separation, have been reported to play critical roles in physiological and pathophysiological processes.<sup>23 24</sup> Forming of protein condensates is of particular interest when occurring in the nucleus, where gene transcription takes place.<sup>25</sup> Notably, our previous study has suggested that NSD2 binds SRC-3 protein and promotes SRC-3 condensation, thus promoting MM drug resistance.<sup>26</sup> Wang *et al* recently report that activation of kinase PYK2 is required for ATRA-induced CD38 upregulation in part of mantle cell lymphoma cells, and PYK2 inhibitor barely

reverses the CD38 upregulation in all cells,<sup>19</sup> which indicates that mechanisms underlying ATRA-induced CD38 upregulation need to be further explored, especially whether protein condensation is involved in the activation of ATRA signaling.

In this study, we aim to evaluate the efficacy of ATRA in upregulating CD38 expression in MM cell lines and primary CD138<sup>+</sup> plasma cells with different genetic backgrounds to elucidate the working machinery, and assess the efficacy of ATRA in promoting anti-CD38 immunotherapies of MM in vitro and in vivo. Our current study discovers a mechanism of ATRA and clarifies its clinical potential for MM immunotherapy.

## METHODS

### Patient samples

Preparation of CD138<sup>+</sup> cells from patients with MM has been described in a previous study.<sup>27</sup>

### Viral vector construction, production, and retroviral transduction

The CD38 CAR sequence was reversely translated and cloned into the lentiviral vector pLTE with an EF1a promoter, and a GFP fluorescent reporter gene was inserted ahead of the CAR sequence. Lentivirus was produced in the HEK293T cells by cotransfection with 12  $\mu$ g psPAX2 vector, 8  $\mu$ g pMD2.G packaging plasmid, and 18  $\mu$ g CD38 CAR vector. Medium was replaced at 24 hours after transfection, and 48 hours viral supernatants were collected and concentrated by ultracentrifugation before infection.

Primary human T cells were isolated using a human T-cell isolation kit and resuspended to  $1 \times 10^7$ /mL density. T cells were activated by Human T-Expander CD3/CD28 Dynabeads at a ratio of 1:1 in T-cell medium (X-VIVO 15 supplemented with 10% fetal bovine serum, 10 mM N-2-hydroxyethylpiperazine-N-2-ethane sulfonic acid (HEPES), 100 U/mL penicillin, 100  $\mu$ g/mL streptomycin, 2 mM L-glutamine, human interleukin (IL)-2 (40 IU/mL), human IL-15 (10 ng/mL), human IL-7 (10 ng/mL) for 3 days. Activated T cells were then lentivirally transduced on day 3 (Multiplicity of infection (MOI)=10, 32°C, centrifugation at  $1000 \times g$  for 1 hour). Supernatants were changed after 12 hours and cells were cultured in 300 IU/mL IL-2. Anti-CD3/CD28 beads were removed on day 5. Media and IL-2 were changed every 2 days. T cells were maintained at  $2 \times 10^6$  cells/mL. Transduction efficiencies were routinely 70%. CAR T cells were used for in vitro assays or transferred into mice on days 10–11 after activation. CD38 CARs were detected with FACS Aria II (BD Bioscience).

### Cell lines and flow cytometry assays

MM cell lines used in our lab have been described in a previous publication.<sup>27</sup> All cells were STR (short tandem repeat) authenticated (Biowing Biotech, Shanghai, China) and mycoplasma-free confirmed with the

Universal Mycoplasma Detection Kit (ATCC, Manassas, Virginia, USA). Flow cytometry was used to detect apoptosis and cytokine production as previously described.<sup>27–29</sup> All antibodies, vendors, dilutions were provided in the supplementary materials. The staining protocol for surface and intracellular antigen has been described in a previous study.<sup>29</sup>

### mRNA and protein assays

RNA extraction, real-time PCR, western blotting, luciferase assay, immunofluorescence staining, in vitro droplet assay and ChIP-qPCR assay were performed as previously described.<sup>27–29</sup> The representative western blot images represent at least three independent experiments.

### Fluorescence recovery after photobleaching (FRAP)

MM cells were subjected to FRAP experiments with an Olympus FV1000 IX81-SIM Confocal Microscope (Olympus, Tokyo, Japan). Photobleaching was performed using tornado mode with the 488 nm laser at 100% laser power for 1–5 s. Enhanced green fluorescent protein (EGFP) fluorescence recovery was monitored with 488 nm laser using the free-run mode at 5 s intervals. Fluorescence of unbleached site in the same view was also monitored as the control. Signal was presented as the ratio relative to the fluorescence signal before photobleaching.

### CAR T-cell proliferation in response to MM cells

CAR T and control T cells were labeled with far-red and cocultured with KMS11 (mixed in 1:1) cells in 96-well plates at  $8 \times 10^4$  cells/well. After 24 hours of incubation, the T-cell proliferation was evaluated via detection of decreasing far-red fluorescence intensity using flow cytometry, and data were analyzed using FlowJo software.

### CAR T efficacy in vitro

Before each assay, T cells were purified using a Pan T Cell Isolation Kit II (Miltenyi Biotec). Ten thousand tumor cells were coincubated with CAR T cells for 6 hours at E:T ratios ranging from 1:20 to 2:1. Cell viability (%) = (CAR T lysis – spontaneous lysis) / (Ctrl T lysis – spontaneous lysis)  $\times 100\%$ . Cytokine production by CAR T cells and CD38 expression by tumor cells were evaluated by coincubation with target tumor cells at a 1:1 ratio ( $10^4$  cells each) for 24 hours. Supernatants were harvested for IFN- $\gamma$  and TNF- $\alpha$  detection using ELISA kit according to the manufacturer's protocol.

### MM mouse model and CAR T-cell activity in vivo

NSG mice (NOD.Cg-Prkdc<sup>scid</sup> ILrg<sup>tm1Wjl</sup>/SzJ) aging 6–12 weeks (n=10/group) were intravenously injected with KMS11<sup>NSD2<sup>+/+</sup></sup> and KMS11<sup>NSD2<sup>+/-</sup></sup>-Luc tumor cell line ( $1 \times 10^6$  cells/mouse) on day 0 to establish the xenograft model. ATRA (10 mg/kg, intraperitoneally) was administered two times a week and mice were randomized into four groups. Mice were intravenously injected with  $5 \times 10^6$  transduced CAR T cells on days 14 and 28; tumor burden was then imaged and evaluated every week at indicated time points. Luminescence images

were analyzed using Living Image software (Caliper Life Sciences). The luciferase signal intensity was quantified using the region of interest (total flux, p/s) with Living Image V.2.50.1 software. Blood was collected from the tail vein, and levels of human IFN- $\gamma$  and TNF- $\alpha$  in serum from each group were measured using ELISA kit (Proteintech, USA). Mouse survival was monitored every week. Mice were killed according to animal protection rules. Kaplan-Meier estimates were used to calculate survival rates.

### Statistical analysis

Data are shown as mean  $\pm$  SD for at least three independent experiments. Differences between groups were determined using paired two-tailed Student's t-test or one-way analysis of variance. Pearson correlation test was used to determine the correlations between gene expressions, and survival analysis was done by GraphPad Prism V.5.0. A p value less than 0.05 was considered statistically significant (\*, p $\leq$ 0.05; \*\*, p $\leq$ 0.01, \*\*\*, p $\leq$ 0.001, compared with the controls, respectively).

## RESULTS

### Effect of ATRA on CD38 expression is t(4;14) dependent in MM cells

To evaluate the effect of ATRA on expressions of common antigens in MM cells, including CD38, BCMA, CD138 and SLAMF7, we treated three widely used MM cell lines, MM.1S, LP-1, and KMS11, with different concentrations of ATRA for 24 hours. Our results showed that expression of CD38, but not other antigens, was markedly augmented at a very low dosage (5 nM) (online supplemental figure S1A). We next used six more cell lines, including U266, RPMI8226, MM.1S, LP-1, KMS11, and OPM2, that have quite different genetic backgrounds to confirm the effect of 5 nM ATRA on CD38 expression. Intriguingly, we found that CD38 expression was elevated in all these cells but was significantly higher in LP-1, KMS11, and OPM2 cells (figure 1A,B) that harbor t(4;14) chromosomal abnormalities. Notably, the effect of ATRA on CD38 expression was obvious only in MM cells harboring t(4;14) translocation (figure 1C, upper panel) but not in MM cells without t(4;14) translocation (figure 1C, lower panel). The phenotype of ATRA on CD38 mRNA expression was also validated (figure 1D and online supplemental figure S1B). In addition, five representative samples from patients with MM showed that ATRA treatment triggered even obvious CD38 expression in NSD2<sup>high</sup> CD138<sup>+</sup> plasma cells compared with NSD2<sup>low</sup> ones (figure 1E), and a significant positive correlation was elicited between NSD2 mRNA and CD38 mRNA upregulation induced by ATRA (figure 1F), while baseline NSD2 had no correlation with CD38 (figure 1G). Collectively, these data suggest that effect of ATRA on CD38 expression is NSD2 dependent.



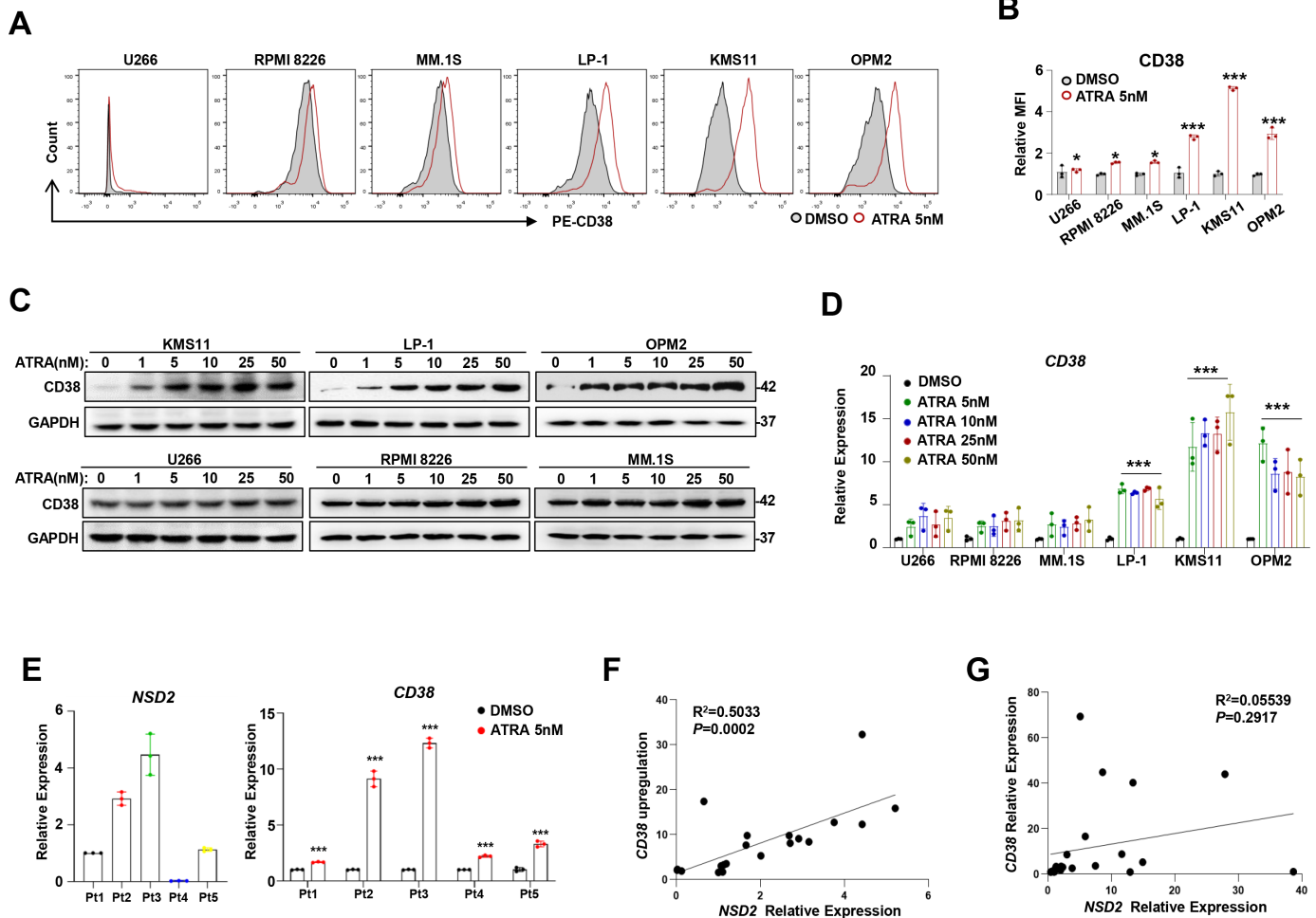


**Figure 1** ATRA-induced CD38 upregulation on MM cells correlates with NSD2 expression. Flow cytometry histograms representing cell surface expression of CD38 on different MM cell lines before and after 5 nM ATRA treatment for 24 hours. (B) Flow cytometry of the MFI in the aforementioned cells. (C) Representative images of western blotting showing CD38 levels in myeloma cell lines on treatment with 1 nM, 5 nM, 10 nM, 25 nM, 50 nM ATRA. (D) qPCR shows CD38 expression in serious myeloma cells treated with increasing concentrations of ATRA for 24 hours. All data represent results from at least three independent experiments, Two-sided p values were determined by Student's t-test; mean $\pm$ SD. (E) NSD2 expressions and ATRA induced CD38 upregulation in CD138<sup>+</sup> plasma cells from representative five patients with MM. (F) The correlation coefficient between the NSD2 expression and ATRA induced CD38 upregulation in CD138<sup>+</sup> MM cells from patients with MM (n=22 samples); (G) The correlation coefficient between the NSD2 and CD38 expression in CD138<sup>+</sup> MM cells from patients with MM (n=22). P values were determined by Pearson coefficient and log-rank test. \*P<0.05, \*\*\*P<0.001. ATRA, all-trans retinoic acid; MFI, mean fluorescence intensity; MM, multiple myeloma; qPCR, quantitative PCR.

### NSD2 directly binds and stabilizes RAR $\alpha$ protein

To further define the mechanism of ATRA induced CD38 expression, we screened the expression of retinoid A receptors, RAR $\alpha$ , RAR $\beta$  and RAR $\gamma$ , as well as retinoid X receptors, RXR $\alpha$ , RXR $\beta$  and RXR $\gamma$  in KMS11 and LP-1 cells treated with ATRA. Expression of RAR $\alpha$ , but not other receptors, was markedly elevated due to 5 nM ATRA treatment (figure 2A), which was also evidenced at protein level (figure 2B). These data suggest ATRA exerts its function mainly through RAR $\alpha$ . In addition, when NSD2 expression was rescued in the KMS11<sup>NSD2<sup>-/-</sup></sup> cells, CD38 expression was boosted according to ATRA treatment (figure 2C). Actually, expression of RAR $\alpha$  was increased in a dose-dependent manner in HEK293T cells ectopically overexpressing NSD2 (figure 2D). Furthermore, knockdown of NSD2, RAR $\alpha$  level, but not

RAR $\beta$ , was evidently suppressed in LP-1 and KMS11 cells compared with their non-target controls (figure 2E).

To further explore the relationship of RAR $\alpha$  and NSD2, we ectopically expressed the NSD2-flag or RAR $\alpha$ -HA protein in HEK293T cells and immunoprecipitated the NSD2 or RAR $\alpha$  protein, respectively, to determine the protein-protein interaction. We found RAR $\alpha$  and NSD2 protein interacts with each other (figure 2F). Accordingly, interaction between endogenous RAR $\alpha$  and NSD2 was also validated by immunoprecipitation assays in LP-1 and KMS11 cells (figure 2G). Remarkably, immunofluorescence staining showed RAR $\alpha$  and NSD2 were mainly colocalized in the nucleus (figure 2H), and the RAR $\alpha$  degradation was significantly postponed according to NSD2 overexpression in MM cells (figure 2I), since the half-life of RAR $\alpha$  protein was obviously augmented

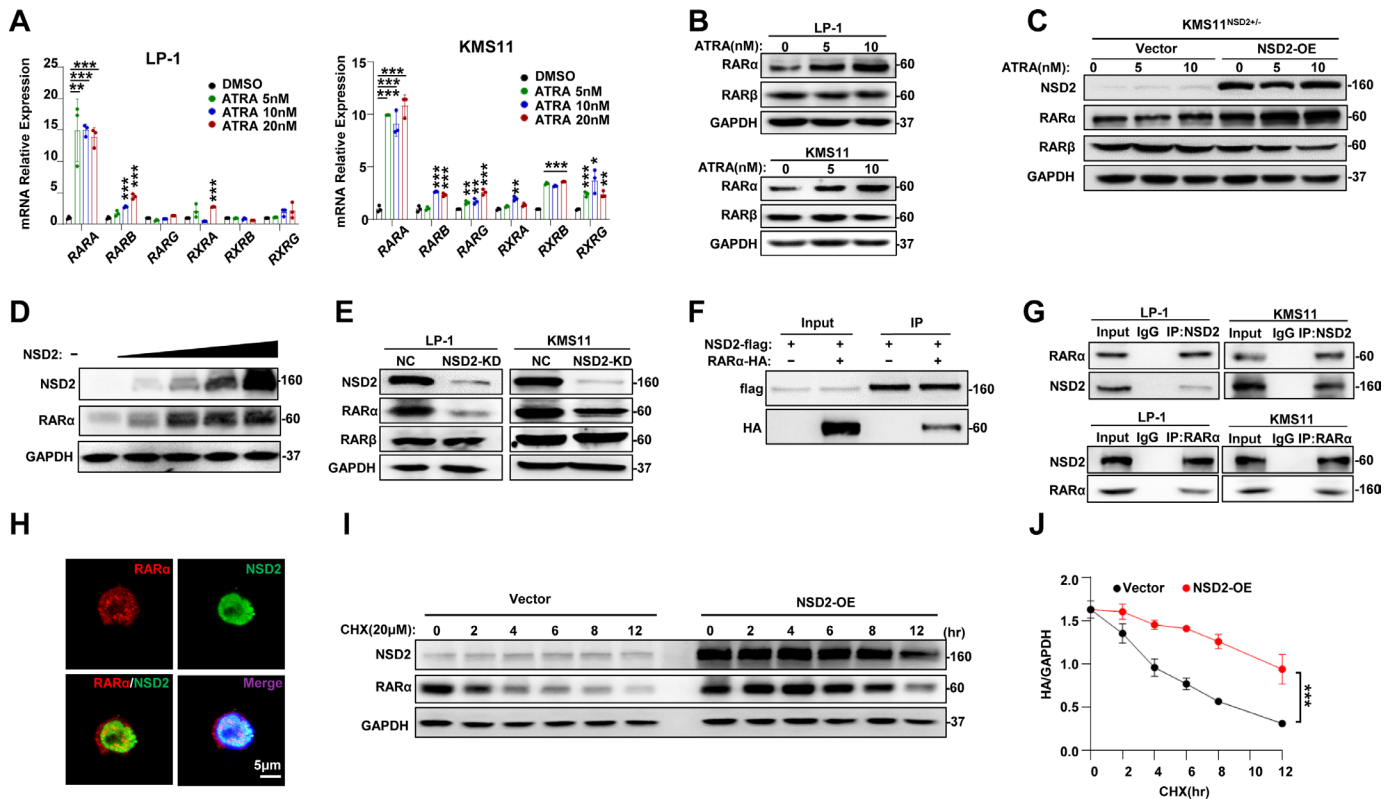


**Figure 2** RAR $\alpha$  physically interacts with NSD2 in myeloma and is correlated with ATRA signaling. (A) qPCR to detect the expressions of ATRA receptor genes in ATRA-treated LP-1 and KMS11 cells. (B) Protein level of RAR $\alpha$  and RAR $\beta$  after ATRA treatment in LP-1 and KMS11 cells. (C) KMS11<sup>NSD2+/-</sup> cells were infected with lentivirus carrying NSD2-OE plasmid or vector control for 72 hours and the NSD2, RAR $\alpha$  and RAR $\beta$  proteins were detected using the western blotting assay. (D) Levels of NSD2 and RAR $\alpha$  protein in HEK293T cells with increasing overexpression of NSD2 by western blotting assay. (E) LP-1 and KMS11 cells infected with lentivirus carrying CRISPR/cas9-NSD2 sgRNA for 72 hours, and the NSD2, RAR $\alpha$  and RAR $\beta$  proteins were detected using western blotting assay. (F) Co-IP to detect the interaction between exogenous NSD2 and RAR $\alpha$  in HEK293T cells transfected with Flag-NSD2 and HA-RAR $\alpha$  for 48 hours. (G) Endogenous NSD2 and RAR $\alpha$  interaction in LP-1 and KMS11 cells using NSD2 Ab or reversely RAR $\alpha$  Ab for immunoprecipitation. (H) IF staining of RAR $\alpha$  (Alexa Fluor 555-conjugated) and NSD2 (Fluorescein isothiocyanate (FITC)-conjugated) in KMS11 cells to show the subcellular colocalization. (I) KMS11<sup>NSD2+/-</sup> cells were infected with lentivirus expressing NSD2 plasmid for 72 hours, and degradation of NSD2 protein within 12 hours with the presence of 20  $\mu$ M CHX was monitored using western blotting assay. (J) Calculated half-life of NSD2 protein in the myeloma cells shown previously. All data represent results from at least three independent experiments. \* $P < 0.05$ ; \*\* $P < 0.01$ ; \*\*\* $P < 0.001$ . Ab, antibody; ATRA, all-trans retinoic acid; CHX, cycloheximide; Co-IP, coimmunoprecipitation; IF, immunofluorescence; NSD2-OE, NSD2-overexpression; qPCR, quantitative PCR.

(figure 2J). These results strongly indicate that NSD2 plays a critical role in activation of ATRA-RAR $\alpha$  signaling.

### NSD2 promotes RAR $\alpha$ phase separation

Interestingly, when predicting the RAR $\alpha$  protein structure for phase separation property, we found two intrinsically disordered regions (IDRs) with very high strength (IDR1, 1–97 amino acids, average strength=0.8066; IDR2, 362–462 amino acids, average strength=0.8110) (online supplemental figure S2A and figure 3A). To test the importance of the IDR regions for RAR $\alpha$  phase separation, we constructed green fluorescent protein (GFP)-fusion IDR proteins to measure droplet formation (online supplemental figure S2B). Indeed, RAR $\alpha$ -IDR1 and RAR $\alpha$ -IDR2 formatted droplets in vitro (figure 3B), which was evidenced by turbidity assay of the fusion proteins (figure 3C). Moreover, aggregations of RAR $\alpha$ -IDR1 and RAR $\alpha$ -IDR2 formatted droplets were abolished by increasing

concentrations of NaCl (figure 3D), and turbidity of IDRs droplets vanished accordingly (figure 3E). When RAR $\alpha$ -GFP fusion protein was forcedly expressed in HEK293T cells, immunofluorescence staining assay showed the fusion proteins were presented as discrete puncta rather than in a diffused status, and treatment of 1,6-hexanediol remarkably attenuated the formation of GFP-RAR $\alpha$  puncta in live cells (figure 3F). When the puncta were bleached with a 488 nm laser, the dismissed puncta were reassembled quickly (figure 3G), and kinetic recovery of RAR $\alpha$ -GFP fluorescence showed that the majority of RAR $\alpha$ -GFP fluorescence was recovered within 50s (figure 3H). Intriguingly, IDRs deleted RAR $\alpha$ -GFP (RAR $\alpha$ - $\Delta$ IDRs) protein failed to format droplets in vitro (figure 3I), and the RAR $\alpha$ - $\Delta$ IDRs protein showed diffused status in live cells (figure 3J). So far, these data have indicated that the RAR $\alpha$  proteins have phase separation formation property.

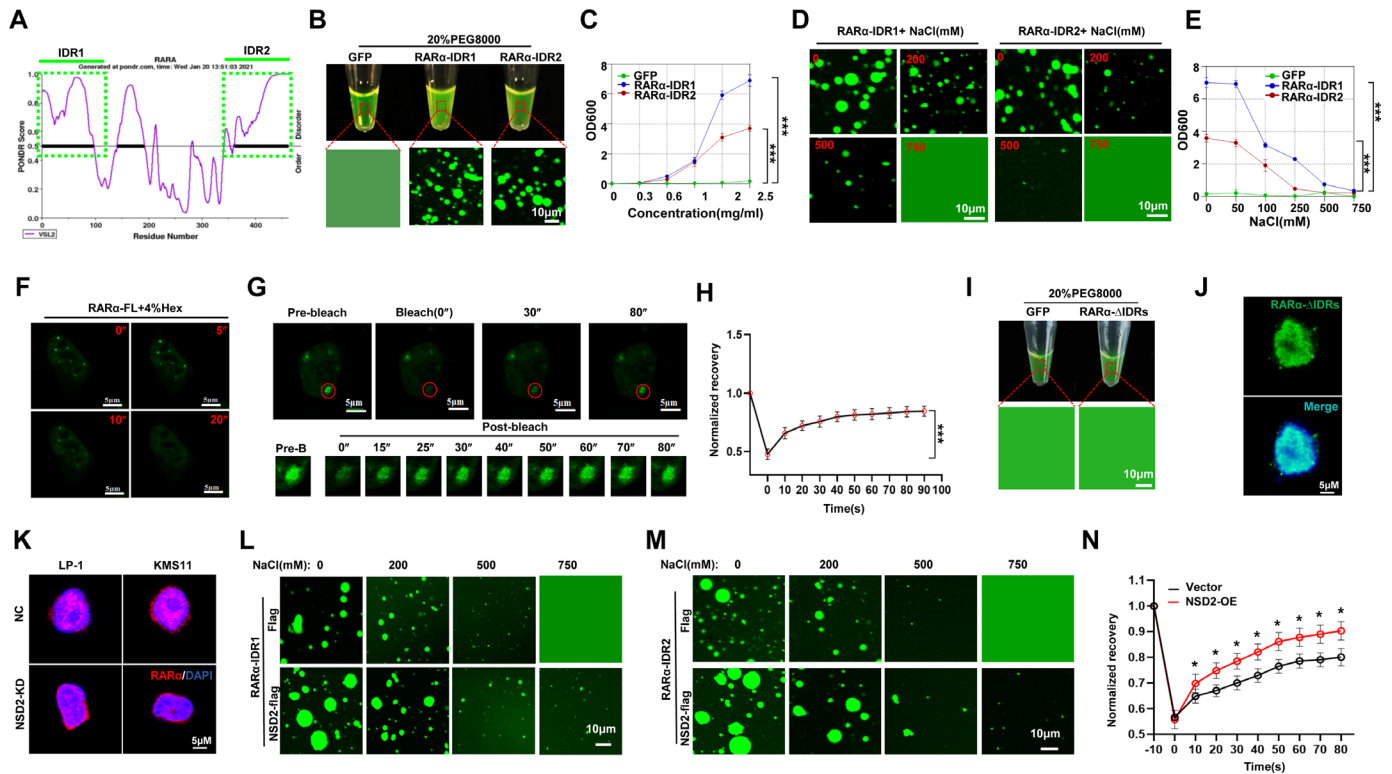


**Figure 3** NSD2 enhances RAR $\alpha$  liquid-liquid phase separation in myeloma cells. (A) Prediction of IDRs (green frame) of RAR $\alpha$  protein using a POND algorithm. (B) Visualization of turbidity associated with droplet formation. Tubes containing GFP (left), GFP-RAR $\alpha$ -IDR1, and GFP-RAR $\alpha$ -IDR2 (middle and right) in the presence of PEG8000. (C) Turbidity (OD600) of GFP-RAR $\alpha$ -IDR1 and GFP-RAR $\alpha$ -IDR2 in 20% PEG. (D) Representative images ( $n=3$  biologically independent experiments) of droplet formation of GFP-RAR $\alpha$ -IDR1 and IDR2 in MM cells at different salt concentrations. GFP-RAR $\alpha$ -IDR1 and IDR2 were added to droplet formation buffer to achieve 5  $\mu$ M protein concentration with a final NaCl concentration as indicated. (E) Turbidity of GFP-RAR $\alpha$ -IDR1 and GFP-RAR $\alpha$ -IDR2 in different salt concentrations as indicated. (F) Phase separation formation of FL GFP-RAR $\alpha$  in MM cells before and after treatment with 4% 1,6-hexanediol at different times. Scale bar, 5  $\mu$ m. (G) FRAP of a RAR $\alpha$ -GFP focus (red framed) by 488 nm laser for 10" bleaching and 90" recovery in KMS11 cells. Scale bar, 5  $\mu$ m. (H) Kinetic recovery times of bleached GFP-fusion RAR $\alpha$  droplet foci in MM cells by 488 nm laser. Two-sided  $p$  values of the comparisons between the final extents of recovery after photobleaching were performed using one-way analysis of variance; mean $\pm$ SD. (I) Visualization of turbidity associated with droplet formation. Tubes containing GFP (left) and GFP-RAR $\alpha$ - $\Delta$ IDRs (right) in the presence of PEG8000 (J) KMS11 cells were infected with lentivirus carrying GFP-RAR $\alpha$ - $\Delta$ IDRs-over expression plasmid for 72 hours and the GFP-fusion protein were detected using IF. (K) Representative images for endogenous foci of RAR $\alpha$  in vector control and NSD2 KD KMS11 and LP-1 cells. Scale bar, 5  $\mu$ m. (L,M) Representative images of droplet formation of GFP-fusion RAR $\alpha$ -IDR1 and IDR2 with 5  $\mu$ M protein concentration in the presence or absence of NSD2 at different NaCl concentrations as indicated. (N) Kinetic recovery times of bleached GFP-fusion RAR $\alpha$  droplet foci in HEK293T cotransfected with NSD2 expressing vector (NSD2-OE) or sgRNA (NSD2 KD) by 488 nm laser ( $n=3$  biologically independent experiments). Two-sided  $p$  values of the comparisons between the final extents of recovery after photobleaching were performed using one-way analysis of variance; mean $\pm$ SD. FL, full length; FRAP, fluorescence recovery after photobleaching; GFP, green fluorescent protein; IDR, intrinsically disordered region; IF, immunofluorescence; KD, knocked-down; MM, multiple myeloma.

Our previous study reported that NSD2 interacts with SRC-3 and promotes its phase separation,<sup>30</sup> so next, we question whether NSD2 has any impact on RAR $\alpha$  phase separation. We found RAR $\alpha$  puncta were obviously decreased in the KMS11 and LP-1 cells when NSD2 was knocked down (figure 3K). Akin to the previous results, exogenously expressed NSD2-flag protein (online supplemental figure S2C) obviously postponed the abolishment of GFP-RAR $\alpha$ -IDR formatted droplets when treated with increasing dosage of NaCl (figure 3L and M). Moreover, when NSD2 was overexpressed, the reassembly of RAR $\alpha$ -GFP puncta bleached by 488 nm laser was significantly enhanced (figure 3N), whereas this process was evidently

suppressed due to NSD2 knockdown in HEK293T cells (online supplemental figure S2D). Collectively, these data strongly suggest that RAR $\alpha$  possesses the property of phase separation, and NSD2 robustly promotes the phase separation of RAR $\alpha$ .

### RAR $\alpha$ phase separation promotes CD38 transcription

Next, we evaluated the importance of RAR $\alpha$  nuclear condensation in ATRA-induced CD38 expression. We ectopically expressed full-length RAR $\alpha$  (RAR $\alpha$ -FL) or IDRs deleted RAR $\alpha$  (RAR $\alpha$ - $\Delta$ IDRs) in KMS11 and LP-1 cells that have been depleted with endogenous RAR $\alpha$ , and flow cytometry analysis showed that CD38 expression due



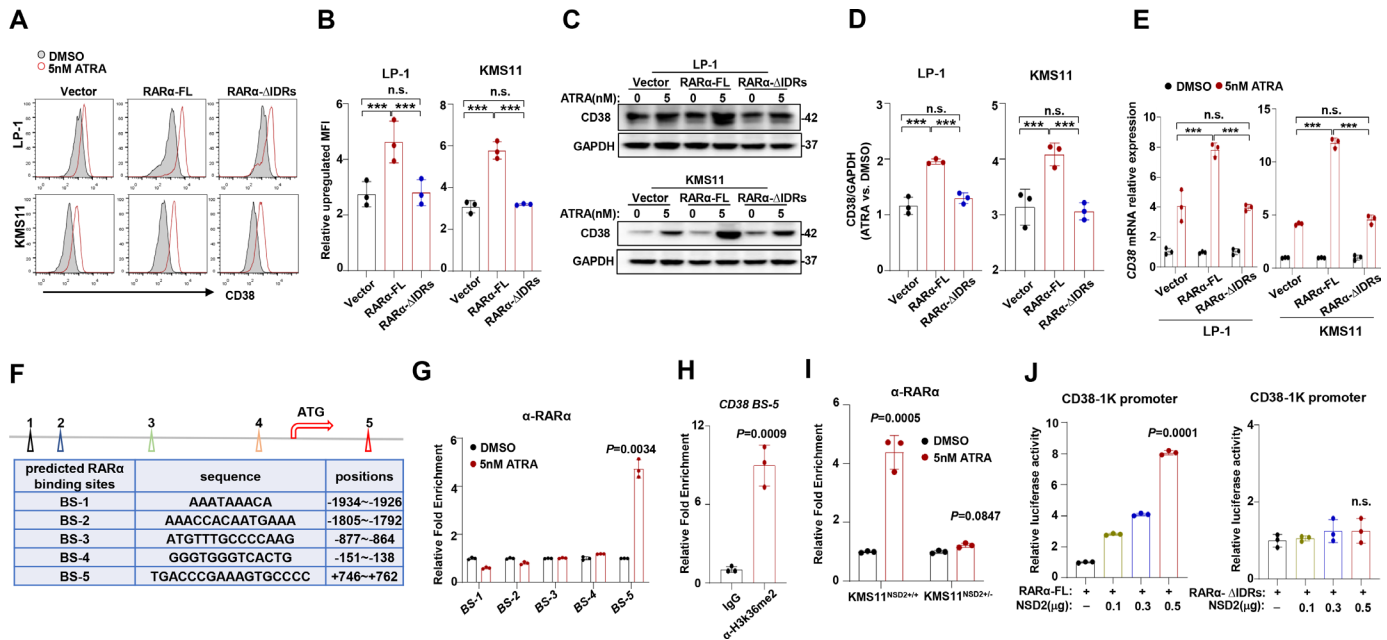


**Figure 4** Condensation of RARα upregulates H3K36me2 modification and CD38 expression. (A,B) Flow cytometry assay analyzing of relative upregulated CD38 MFI in LP-1 and KMS11 cells transfected with vector, RARα-FL, and RARα-ΔIDRs virus induced by 5 nM ATRA for 24 hours and analyzes the difference between groups (n=3). (C,D) Western blot of CD38 expression in LP-1 and KMS11 cells transfected with vector, RARα-FL and RARα-ΔIDRs virus and induced by 5 nM ATRA for 24 hours and analyzes the difference density of according to gray scale densities between groups by ImageJ. (E) Relative upregulated CD38 in LP-1 and KMS11 cells by ATRA of each groups mentioned earlier. (F) Diagram representation predicted RARα BS on the CD38 region. (G) ChIP-qPCR analysis of relative RARα recruitment at CD38 BS region in KMS11 cells after 5 nM ATRA treatment (n=3). PCR primers were designed according predicted RARα BSs of CD38. (H) ChIP-qPCR to detected H3K36me2 modification on the BS. (I) ChIP-qPCR analysis of relative RARα recruitment in the KMS11<sup>NSD2+/+</sup> and KMS11<sup>NSD2+/-</sup> cells after 5 nM ATRA treatment for 24 hours (n=3). (J) The luciferase assay of CD38-promoter in RARα-FL or RARα-ΔIDRs overexpressing cells transfected with increasing amount of NSD2 plasmid. Two-sided p values were determined by Student's t test; mean±SD. \*P<0.05, \*\*P<0.01, \*\*\*P<0.001. ATRA, all-trans retinoic acid; BS, binding site; ChIP, chromatin immunoprecipitation; H3K36me2, histone H3 dimethylation at lysine 36; IDR, intrinsically disordered region; n.s., not significant; qPCR, quantitative PCR.

to ATRA treatment was only enhanced in cells expressing RARα-FL but not RARα-ΔIDRs (figure 4A,B), which were also evidenced at protein level (figure 4C,D) and mRNA level (figure 4E). To further elucidate transcriptional features of RARα that may be responsible for ATRA response, we employed bioinformatics analysis and found there are five predicted RARα binding sites (BSs) on CD38 promoter (figure 4F). Chromatin immunoprecipitation (ChIP)-quantitative PCR (qPCR) assay indicated that ATRA significantly augmented the binding of RARα on the fifth BS (figure 4G). Notably, CD38 was also tightly regulated by histone H3 dimethylation at lysine 36 (H3K36me2), an active transcription modification<sup>31</sup> on the same site after ATRA stimulation (figure 4H), which is catalyzed by NSD2. Indeed, increased enrichment of RARα on CD38 promoter due to ATRA treatment was only detected in KMS11<sup>NSD2+/+</sup> but not in KMS11<sup>NSD2+/-</sup> cells (figure 4I). We next transfected an CD38-luciferase reporter, together with RARα-FL or RARα-ΔIDRs-expressing vectors, in the presence of ATRA in HEK293T cells and found that ascending NSD2 increased CD38 transcriptional activity at a dose-dependent manner only in RARα-FL-expressing cells but not RARα-ΔIDRs-expressing ones (figure 4J). Taken together, these results demonstrate that RARα nuclear condensation recruiting

NSD2 to modify chromatin and promote CD38 transcription activity.

### ATRA enhances antihuman CD38 CAR T-cell therapy for MM cells

Given that ATRA is prone to augment CD38 expression in NSD2<sup>high</sup> cells, we hypothesize that ATRA could enhance the killing efficiency of anti-CD38 CAR T cells for MM cells. To verify this hypothesis, we generated anti-CD38 CAR T cells, which is composed of GFP, single-chain variable fragment (scFv), a transmembrane domain, signaling motifs consisting of CD28 and CD3ζ chain stimulation signaling domains (figure 5A). After being transduced by lentivirus and sorted by fluorescence activated cell sorting (FACS), percentage of GFP<sup>+</sup> human peripheral blood T cell-derived CAR T cells was approximately 98% (online supplemental figure S3A). Transgene-positive CD3<sup>+</sup> T cells were expanded for effector function analysis, compared with CD3<sup>+</sup> T cells transduced with non-GFP-vectors. When cocultured with KMS11 cells, CAR T cells exhibited specific proliferation (online supplemental figure S3B) and lytic activity (figure 5B,C) against MM cell lines, and anti-CD38 CAR T cells exerted tumor killing effect in an effector-to-target (E:T) ratio-dependent manner (figure 5D). Moreover, significant

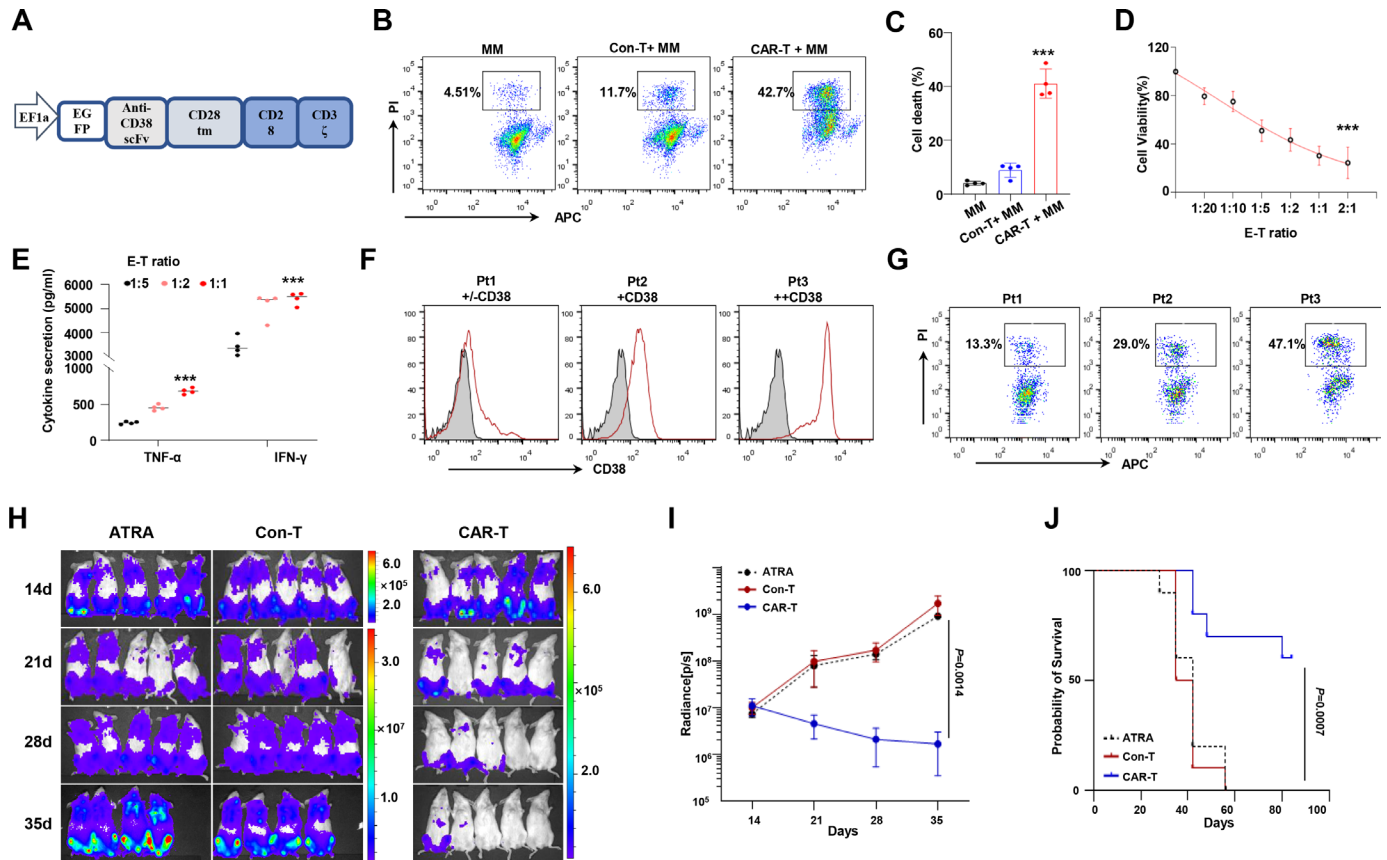


**Figure 5** CD38-CAR construct and CD38-CAR T-cell phenotype. Schematic representation of the CD38 CAR construct. The second-generation CAR includes a SP, an anti-CD38 scFv with a GFP-tag, an IgG1 CH2-CH3 hinge, a CD28 tm region, a CD28 cytoplasmic portion, and the cytoplasmic portion of the CD3ζ activation domain. (B,C) In vitro cytotoxicity of CD38 CAR T cells or Con-T cells against MM cells was determined by flow cytometry. Data represent mean±SD of three independent experiments. (D) On coculture with MM cells at E:T cell ratios of 1:20, 1:10, 1:5, 1:2, and 2:1, CAR T cells showed increasing antitumor effect. \*\*\*P<0.001. (E) IFN-γ and TNF-α in the supernatant were detected by ELISA. All data represent results from at least three independent experiments. (F,G) Antitumor effects of the anti-CD38 CAR T against patients with CD138<sup>+</sup> MM cells with various CD38 levels. (H) Antitumor effects of the anti-CD38 CAR T cells in NSG mice intravenously injected with  $1 \times 10^6$  Luc-transduced KMS11 cells, T cells carrying vector or ATRA injected mice were used as control (n=5/group); a series of bioluminescent imaging results showing myeloma progression in mice is shown. (I) Total flux of whole-body bioluminescence measured using in vivo imaging system (IVIS) is shown as mean±SEM. (J) Survival rate of each group of mice at indicated time point (n=10 mice per group). Two-sided p value was analyzed in CAR-T and Con-T group using log-rank test. CAR, chimeric antigen receptor; Con-T, control T; E:T, effector-to-target; GFP, green fluorescent protein; IFN-γ, interferon gamma; MM, multiple myeloma; NSG, NOD.Cg-Prkdc<sup>scid</sup>Il2rg<sup>tm1Wjl</sup>/SzJ; scFv, single-chain variable fragment; SP, signal peptide; tm, transmembrane; TNF-α, tumor necrosis factor alpha.

production of interferon gamma (IFN-γ) and tumor necrosis factor alpha (TNF-α) by the CAR T cells was detected (figure 5E). The impact of CD38 expression levels on anti-CD38 CAR T-cell-mediated killing efficiency was also elicited in primary CD138<sup>+</sup> cells from patients with MM with various levels of CD38 expression (figure 5F,G). The in vivo effects of anti-CD38 CAR T cells were evaluated in the NOD.Cg-Prkdc<sup>scid</sup>Il2rg<sup>tm1Wjl</sup>/SzJ (NSG) mice intravenously inoculated with  $1 \times 10^6$  KMS11-Luc cells. After  $5 \times 10^6$  CAR T cells were administered at days 14 and 28, we found that tumor growth was significantly inhibited compared with control (figure 5H,I), and the overall survival of mice also improved obviously (p=0.0007) (figure 5J). Collectively, all these data indicate that our anti-CD38 CAR T cells exert effective antitumor activity.

To evaluate whether ATRA promotes anti-CD38 CAR T-cell-mediated immunotherapy for MM cells is NSD2 dependent, we treated KMS11<sup>NSD2+/+</sup> and KMS11<sup>NSD2+/-</sup> cells with 5nM ATRA or Dimethyl Sulfoxide (DMSO) vehicle for 24 hours and then incubated these cells with anti-CD38 CAR T cells. We found under different E:T ratios that ATRA treatment induced limited cell death in KMS11<sup>NSD2+/-</sup> cells but considerably augmented cell death in KMS11<sup>NSD2+/+</sup> cells (figure 6A-C). Further analyzing CAR T function by flow cytometry or ELISA, we observed notably elevated proinflammatory cytokines in anti-CD38 CAR T cells cocultured with KMS11<sup>NSD2+/+</sup> cells but not with KMS11<sup>NSD2+/-</sup> (figure 6D and E, and online supplemental figure S3C). Using in vivo NSG mice bearing KMS11-Luc model for MM (figure 6F), we treated the mice with ATRA or vehicle two times a week



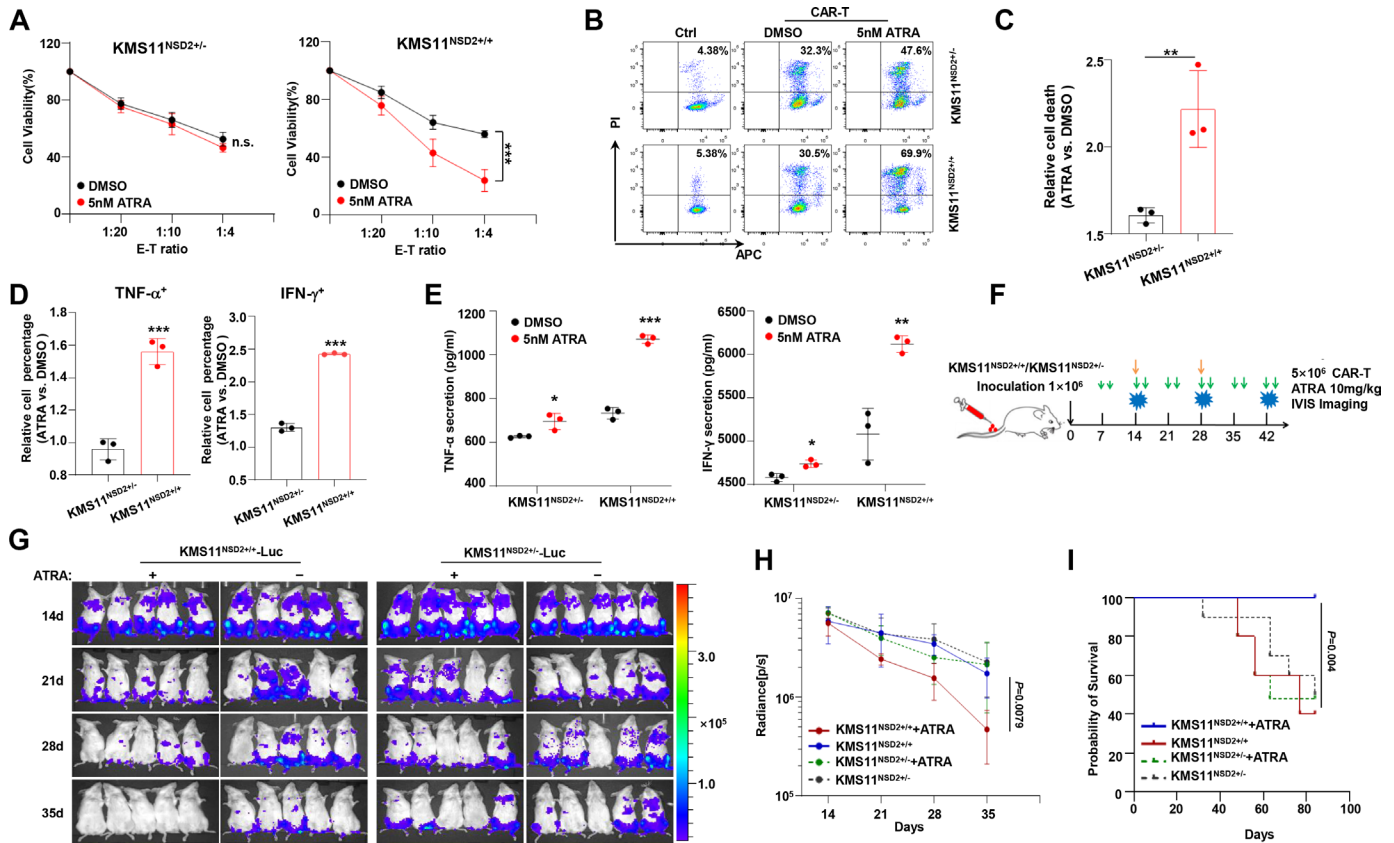


**Figure 6** ATRA improves response to CD38 CAR T in vivo and in vitro. (A) Cytotoxicity assay of CD38-CAR T cells against KMS11<sup>NSD2+/+</sup> or KMS11<sup>NSD2+/-</sup> cells at three different E:T ratios. (B) Evaluation of KMS11<sup>NSD2+/+</sup> or KMS11<sup>NSD2+/-</sup> cells death after coculturing with CD38-CAR T at an E:T ratio of 1:4 by flow cytometry. (C) Flow cytometry analysis of cell death in the KMS11<sup>NSD2+/+</sup> or KMS11<sup>NSD2+/-</sup> cells after ATRA treatment (n=3). (D) Analysis of fold change of IFN- $\gamma$ <sup>+</sup> and TNF- $\alpha$ <sup>+</sup> CAR T percentage after ATRA treatment in the KMS11<sup>NSD2+/+</sup> or KMS11<sup>NSD2+/-</sup> cells. (E) Determination of IFN- $\gamma$  and TNF- $\alpha$  secretion by ELISA in coculture supernatant. (F) Schematic of CAR T cell and ATRA treatment protocol. (G) Images of representative mice per treatment group. (H) Analysis of tumor load per treatment group (n=10 mice per group). Arrows indicate the time when ATRA and CAR T treatment began (days 7 and 14). Differences between groups were analyzed using one-way analysis of variance. (I) Survival rate of each group of mice at indicated time point (n=10 mice per group). Two-sided p values were analyzed using log-rank test. ATRA, all-trans retinoic acid; CAR, chimeric antigen receptor; E:T, effector-to-target; IFN- $\gamma$ , interferon gamma; TNF- $\alpha$ , tumor necrosis factor alpha. \*P<0.05, \*\*P<0.01, \*\*\*P<0.001.

from 1 week and found ATRA could upregulate expression of CD38 on KMS11<sup>NSD2+/+</sup> MM cells in vivo but not KMS11<sup>NSD2+/-</sup> MM cells (online supplemental figure S3D). When aggressive tumors were developed at day 14, we injected  $5 \times 10^6$  anti-CD38 CAR T cells or control cells into mice. As shown in figure 6G, ATRA significantly reinforced the antitumor effect of anti-CD38 CAR T cells for mice injected with KMS11<sup>NSD2+/+</sup> MM cells, but no obvious change was elicited in mice bearing KMS11<sup>NSD2+/-</sup> MM cells (figure 6G). Obviously, the combination of ATRA and anti-CD38 CAR T cells exerted a prominent anti-MM effect on KMS11<sup>NSD2+/+</sup> MM cells in vivo, evidenced by significantly reduced luminescence signal (figure 6H) and meaningfully prolonged survival rate (figure 6I). These data strongly support our hypothesis that ATRA improves the efficacy of anti-CD38 CAR T cells against NSD2<sup>high</sup> MM.

## DISCUSSION

Despite promising response rates, low levels of CD38 on a subset of tumor cells, loss of CD38, and outgrowth

of CD38<sup>+</sup> tumor cells have been suggested as a major obstacle in managing RRMM in the clinic. Previous studies have discovered ATRA enhances the expression of CD38 antigen, but the working machinery and genomic background that correlate with ATRA sensitivity remain an obstacle. In the present study, we discover that ATRA is prone to promote CD38 expression in MM cells harboring t(4;14) translocation, since this kind of chromatin abnormality gendered histone methyltransferase NSD2 interacts with ATRA receptor RAR $\alpha$ , consequentially stabilizes RAR $\alpha$  protein, and enhances phase separation of RAR $\alpha$ . Notably, our study also highlights the effect of ATRA in enhancing therapeutic efficiency of anti-CD38 CAR T cells in the NSD2<sup>high</sup> MM.

It is widely recognized that effective antigen density is of great importance in the determination of CAR T-cell efficacy.<sup>32-34</sup> For example, a previous study demonstrated that low expression of target antigen contributes to limited antitumor efficacy of the ALK CAR.<sup>33</sup> Xenograft models

of B-ALL also demonstrated that the capacity for the CD22 CAR to produce cytokine and control tumor cells was exquisitely dependent on surface expression levels of CD22.<sup>35</sup> Unfortunately, loss of antigen and outgrowth of antigen-negative tumor cells have been reported in many cases after CAR T therapy.<sup>34</sup> Actually, the initial clinical trials for CAR T cells targeting CD38 have adopted stringent criteria for CD38 surface expression (over 50% CD38<sup>+</sup>) for patient enrollment,<sup>8</sup> and a recent study using small molecule to augment BCMA expression has elicited susceptibility to anti-BCMA CAR T cells in MM in vitro and in vivo, and an Food and Drug Administration-approved clinical trial has been initiated (NCT03502577). ATRA has been reported to exert synergistic and additive effects in combination with different antitumor therapies.<sup>36</sup> We find that, among several common CAR T target antigens, CD38 is the most obviously upregulated one in several MM cells harboring t(4;14) translocation. Importantly, we find that the effect of ATRA on CD38 expression is non-linear dependence, since 5 nM ATRA has a similar effect with 100 nM dosage. Similar with our results, Wang *et al* also disclose that expression of CD38 barely shows time dependence or dose dependence.<sup>19</sup> These results strongly suggest that the mechanism underlying ATRA inducing CD38 expression is not well clarified.

T(4;14) translocation is one of the high risks that confer poor prognosis for MM, and patients bearing this chromatin abnormality often suffer from chemoresistance to current regimens. We find that upregulation of CD38 by ATRA is more significantly in the t(4;14) MM cells, and this effect attenuates when NSD2 is deficit. The t(4;14) translocation confers high expression of histone methyltransferase NSD2,<sup>37</sup> which specifically catalyzes H3K36 dimethylation (H3K36me2).<sup>38</sup> Specifically, we find that NSD2 interacts and stabilizes RAR $\alpha$  and leads to H3K36me2 modification on *CD38* promoter and facilitates its expression. Thus, results from this study suggest that when using anti-CD38 CAR T-cell therapy and ATRA for t(4;14) patients with MM, we do not have to exclude those with low CD38 expression at baseline. ATRA may also be considered for patients with t(4;14) with low or losing antigen after CD38-targeted therapies. Our results indicate that treating patients with t(4;14) with ATRA to increase expression of the target antigen could overcome low antigen density, thus improving therapy efficacy of CAR T cells. Clinical application of the combination could be beneficial in these patients, accounting for 11% of all patients with MM.<sup>1</sup> However, effects of ATRA on CD38-targeted therapies beyond this high-risk group need further investigation. Alternatively, CAR could be engineered to enhance response to low antigen densities. The most commonly attempted modification has been to enhance the affinity of the ScFv for its target. Notably, though ATRA was reported to enhanced the antitumor activity of daratumumab in xenograft tumors by elevating CD38 expression,<sup>19</sup> the combination of daratumumab with ATRA has limited activity in patients with daratumumab refractory MM.<sup>39</sup> The discrepancy could

be explained by the fact that CD38 downregulation is not the only reason of resistance to CD38 antibodies. Daratumumab has completely different modes of action compared with CAR T, including complement-mediated cytotoxicity, Ab-dependent cellular phagocytosis, and Ab-dependent cellular cytotoxicity,<sup>40</sup> which are largely dependent on BM niche. In daratumumab refractory MM, natural killer cell dysfunction<sup>41</sup> and T-cell exhaustion<sup>42</sup> have been developed; increased levels of complement inhibitors<sup>43</sup> also hampered daratumumab efficacy. In addition, the aforementioned studies did not classify patients according to genomic backgrounds, such as t(4;14), which is of the main revelation of the current study.

One consequence of protein–protein interactions is to form phase separation, and the IDRs of proteins are key elements to form condensation.<sup>44</sup> The condensed protein compartmentalizes transcription apparatus and exerts augmented biological functions compared with their diffused compartment,<sup>23 26 30 45 46</sup> which may explain why ATRA stimulates CD38 expression in a non-linear manner. Despite ample studies concerning the ATRA signaling pathway having been widely discussed over the past decades, the phase separation property and significance of RAR $\alpha$  in tumors have not been noticed. Our present study provides evidence that RAR $\alpha$  has two IDRs and has the property of forming phase separation, and the interaction with NSD2 enhances this condensation. Specifically, we disclose that RAR $\alpha$  nuclear condensation recruits NSD2 to exert H3K36me2 modifications on *CD38* promoter, therefore enriching *CD38* expression on ATRA stimulation. Indeed, in CD138<sup>+</sup> plasma cells from patients with MM, upregulation of CD38 can only be triggered in those with high expression of NSD2 on ATRA stimulation. Our present findings provide mechanistic insights in understanding how genomic background determines sensitivity of MM to ATRA, and the clinical relevance of our results is that when using ATRA to enhance anti-CD38-based immunotherapies, genomic backgrounds should be taken into consideration. However, our results also indicate that ATRA promotes the transcription level of *RARA*; whether this is a self-activation by RAR $\alpha$  phase separation or through other pathways triggered by ATRA has not been discussed in the current study.

Several clinical trials used ATRA in combination with chemotherapy for patients with cancer.<sup>47 48</sup> Though it is quite complicated to convert drug concentration from in vitro to in vivo, clinical trials showed 45 mg/m<sup>2</sup> ATRA in combination with daratumumab for patients with MM (NCT02751255) does not increase the incidence of adverse events. We choose 10 mg/kg body weight for mice (20 g, 36 cm<sup>2</sup>) in our study. A previous study<sup>49</sup> suggested that CD38 was upregulated in CD34<sup>+</sup> cells by 100 nM ATRA treatment in vitro, but the effect in vivo is not mentioned. Our results indicate that ATRA could not increase CD38 expression on CD34<sup>+</sup> cells, and the percentage of CD34<sup>+</sup> cells in BM was not statistically changed under this concentration in vivo (online

supplemental figure S3E,F). The dose of ATRA should be carefully evaluated when used clinically to improve efficacy of CAR T therapy.

In conclusion, we disclose the important role of NSD2 in mediating ATRA-induced CD38 expression in MM cells, and our study suggests that combination of anti-CD38 CAR T cells with ATRA is a promising approach to improve tumor cell elimination in patients with MM, and ATRA may also be used in non-responder or relapsed patients with t(4;14) after CD38-targeted therapies.

**Contributors** ZL and J-QM designed the project and finalized the manuscript and revision; JW drafted the manuscript; ZP, JW, XL, SW, YX, HJ, and YW performed experiments and statistical analyses; ZP, JW, JG, MH and MW carried out animal studies; QL and YW provided the patient samples and clinical statistics. ZL and J-QM are acting as guarantors.

**Funding** This work was supported by Cancer Biobank of Tianjin Medical University Cancer Institute and Hospital. We thank Dr Yong Lu at Houston Methodist Hospital and Research Institute for construction of CD38 CAR. This work was supported by the Beijing Natural Science Foundation of China (Z200020, ZQL), the National Natural Science Foundation of China (81870161, 82070221, ZQL; 82070227, J-QM ; 81900215, JY Wang; 82270208, YFW; 82000216, QL), and the Shanghai Guangci Translational Medicine Research Foundation.

**Competing interests** None declared.

**Patient consent for publication** Not applicable.

**Ethics approval** This study was approved by the ethics committee of Tianjin Medical University. All protocols were conducted in accordance with the Declaration of Helsinki. Signed informed consent was obtained from all subjects enrolled in this study. Animal studies were approved by the Committee on Animal Research and Ethics of Tianjin Medical University, and all protocols conformed to the Guidelines for Ethical Conduct in the Care and Use of Non-human Animals in Research (TMUaMEC2020016).

**Provenance and peer review** Not commissioned; externally peer reviewed.

**Data availability statement** Data sharing not applicable as no datasets generated and/or analyzed for this study.

**Supplemental material** This content has been supplied by the author(s). It has not been vetted by BMJ Publishing Group Limited (BMJ) and may not have been peer-reviewed. Any opinions or recommendations discussed are solely those of the author(s) and are not endorsed by BMJ. BMJ disclaims all liability and responsibility arising from any reliance placed on the content. Where the content includes any translated material, BMJ does not warrant the accuracy and reliability of the translations (including but not limited to local regulations, clinical guidelines, terminology, drug names and drug dosages), and is not responsible for any error and/or omissions arising from translation and adaptation or otherwise.

**Open access** This is an open access article distributed in accordance with the Creative Commons Attribution Non Commercial (CC BY-NC 4.0) license, which permits others to distribute, remix, adapt, build upon this work non-commercially, and license their derivative works on different terms, provided the original work is properly cited, appropriate credit is given, any changes made indicated, and the use is non-commercial. See <http://creativecommons.org/licenses/by-nc/4.0/>.

#### ORCID iD

Zhiqiang Liu <http://orcid.org/0000-0002-0677-8097>

#### REFERENCES

- Kumar SK, Rajkumar V, Kyle RA, *et al.* Multiple myeloma. *Nat Rev Dis Primers* 2017;3.
- Palumbo A, Anderson K. Multiple myeloma. *N Engl J Med* 2011;364:1046–60.
- Podar K, Leleu X. Relapsed/refractory multiple myeloma in 2020/2021 and beyond. *Cancers (Basel)* 2021;13:5154.
- Dima D, Jiang D, Singh DJ, *et al.* Multiple myeloma therapy: emerging trends and challenges. *Cancers (Basel)* 2022;14:4082.
- Chng WJ, Kuehl WM, Bergsagel PL, *et al.* Translocation T (4; 14) retains prognostic significance even in the setting of high-risk molecular signature. *Leukemia* 2008;22:459–61.
- Pehlivan KC, Duncan BB, Lee DW. CAR-T cell therapy for acute lymphoblastic leukemia: transforming the treatment of relapsed and refractory disease. *Curr Hematol Malig Rep* 2018;13:396–406.
- Ghandili S, Weisel KC, Bokemeyer C, *et al.* Current treatment approaches to newly diagnosed multiple myeloma. *Oncol Res Treat* 2021;44:690–9.
- Gagelmann N, Riecken K, Wolschke C, *et al.* Development of CAR-T cell therapies for multiple myeloma. *Leukemia* 2020;34:2317–32.
- van de Donk NWCJ, Richardson PG, Malavasi F. CD38 antibodies in multiple myeloma: back to the future. *Blood* 2018;131:13–29.
- Liang C, Qiao G, Liu Y, *et al.* Overview of all-trans-retinoic acid (ATRA) and its analogues: structures, activities, and mechanisms in acute promyelocytic leukaemia. *Eur J Med Chem* 2021;220:S0223-5234(21)00300-7.
- Mi J-Q, Chen S-J, Zhou G-B, *et al.* Synergistic targeted therapy for acute promyelocytic leukaemia: a model of translational research in human cancer. *J Intern Med* 2015;278:627–42.
- Ghyselinck NB, Duester G. Retinoic acid signaling pathways. *Development* 2019;146:dev167502.
- Ding X, Wang W, Wang M, *et al.* DOK1/ppargamma pathway mediates anti-tumor ability of all-trans retinoic acid in breast cancer MCF-7 cells. *Biochem Biophys Res Commun* 2017;487:189–93.
- Centrifto F, Paroni G, Bolis M, *et al.* Cellular and molecular determinants of all-trans retinoic acid sensitivity in breast cancer: luminal phenotype and *rxrα* expression. *EMBO Mol Med* 2015;7:950–72.
- Gudas LJ, Wagner JA. Retinoids regulate stem cell differentiation. *J Cell Physiol* 2011;226:322–30.
- Shi J, Zheng B, Chen S, *et al.* Retinoic acid receptor  $\alpha$  mediates all-trans-retinoic acid-induced KLF4 gene expression by regulating KLF4 promoter activity in vascular smooth muscle cells. *J Biol Chem* 2012;287:10799–811.
- Mehta K, McQueen T, Manshuri T, *et al.* Involvement of retinoic acid receptor-alpha-mediated signaling pathway in induction of CD38 cell-surface antigen. *Blood* 1997;89:3607–14.
- Gao Y, Camacho LH, Mehta K. Retinoic acid-induced CD38 antigen promotes leukemia cells attachment and interferon-gamma/interleukin-1beta-dependent apoptosis of endothelial cells: implications in the etiology of retinoic acid syndrome. *Leuk Res* 2007;31:455–63.
- Wang X, Yu X, Li W, *et al.* Expanding anti-CD38 immunotherapy for lymphoid malignancies. *J Exp Clin Cancer Res* 2022;41:210.
- Nijhof IS, Groen RWJ, Lokhorst HM, *et al.* Upregulation of CD38 expression on multiple myeloma cells by all-trans retinoic acid improves the efficacy of daratumumab. *Leukemia* 2015;29:2039–49.
- Mezquita B, Mezquita C. Two opposing faces of retinoic acid: induction of stemness or induction of differentiation depending on cell-type. *Biomolecules* 2019;9:567.
- van Gils N, Verhagen H, Smit L. Reprogramming acute myeloid leukemia into sensitivity for retinoic-acid-driven differentiation. *Exp Hematol* 2017;52:12–23.
- Zhang H, Ji X, Li P, *et al.* Liquid-Liquid phase separation in biology: mechanisms, physiological functions and human diseases. *Sci China Life Sci* 2020;63:953–85.
- Igelmann S, Lessard F, Ferbeyre G. Liquid-Liquid phase separation in cancer signaling, metabolism and anticancer therapy. *Cancers (Basel)* 2022;14:1830.
- Guo C, Luo Z, Lin C. Phase separation properties in transcriptional organization. *Biochemistry* 2022;61:2456–60.
- Sabari BR, Dall'Agnese A, Boija A, *et al.* Coactivator condensation at super-enhancers links phase separation and gene control. *Science* 2018;361:eaar3958.
- Xie Y, Liu J, Jiang H, *et al.* Proteasome inhibitor induced SIRT1 deacetylates Gli2 to enhance hedgehog signaling activity and drug resistance in multiple myeloma. *Oncogene* 2020;39:922–34.
- Liu Z, Xu J, He J, *et al.* A critical role of autocrine sonic hedgehog signaling in human CD138+ myeloma cell survival and drug resistance. *Blood* 2014;124:2061–71.
- Wu Y, Wang X, Lu Y, *et al.* Inpp4B exerts a dual role in gastric cancer progression and prognosis. *J Cancer* 2021;12:7201–13.
- Liu J, Xie Y, Guo J, *et al.* Targeting NSD2-mediated SRC-3 liquid-liquid phase separation sensitizes bortezomib treatment in multiple myeloma. *Nat Commun* 2021;12:1022.
- Sengupta D, Zeng L, Li Y, *et al.* NSD2 dimethylation at H3K36 promotes lung adenocarcinoma pathogenesis. *Mol Cell* 2021;81:4481–92.
- Caruso HG, Heimberger AB, Cooper LJJ. Steering CAR T cells to distinguish friend from foe. *Oncoimmunology* 2019;8:e1271857.
- Walker AJ, Majzner RG, Zhang L, *et al.* Tumor antigen and receptor densities regulate efficacy of a chimeric antigen receptor targeting anaplastic lymphoma kinase. *Mol Ther* 2017;25:2189–201.



- 34 Majzner RG, Mackall CL. Tumor antigen escape from CAR T-cell therapy. *Cancer Discov* 2018;8:1219–26.
- 35 Fry TJ, Shah NN, Orentas RJ, et al. CD22-targeted CAR T cells induce remission in B-ALL that is naive or resistant to CD19-targeted CAR immunotherapy. *Nat Med* 2018;24:20–8.
- 36 Schultze E, Collares T, Lucas CG, et al. Synergistic and additive effects of atra in combination with different anti-tumor compounds. *Chem Biol Interact* 2018;285:69–75.
- 37 Keats JJ, Maxwell CA, Taylor BJ, et al. Overexpression of transcripts originating from the MMSET locus characterizes all T (4; 14) (p16; q32) -positive multiple myeloma patients. *Blood* 2005;105:4060–9.
- 38 Popovic R, Martinez-Garcia E, Giannopoulou EG, et al. Histone methyltransferase MMSET/NSD2 alters EZH2 binding and reprograms the myeloma epigenome through global and focal changes in H3K36 and H3K27 methylation. *PLoS Genet* 2014;10:e1004566.
- 39 Frerichs KA, Minnema MC, Levin M-D, et al. Efficacy and safety of daratumumab combined with all-trans retinoic acid in relapsed/refractory multiple myeloma. *Blood Adv* 2021;5:5128–39.
- 40 van de Donk NWCJ, Usmani SZ. CD38 antibodies in multiple myeloma: mechanisms of action and modes of resistance. *Front Immunol* 2018;9:2134.
- 41 Casneuf T, Xu XS, Adams HC, et al. Effects of daratumumab on natural killer cells and impact on clinical outcomes in relapsed or refractory multiple myeloma. *Blood Adv* 2017;1:2105–14.
- 42 Verkleij CPM, Jhatakia A, Broekmans MEC, et al. Preclinical rationale for targeting the PD-1/PD-L1 axis in combination with a CD38 antibody in multiple myeloma and other CD38-positive malignancies. *Cancers (Basel)* 2020;12:3713.
- 43 Nijhof IS, Casneuf T, van Velzen J, et al. CD38 expression and complement inhibitors affect response and resistance to daratumumab therapy in myeloma. *Blood* 2016;128:959–70.
- 44 Christensen NR, Pedersen CP, Sereikaite V, et al. Bidirectional protein-protein interactions control liquid-liquid phase separation of PSD-95 and its interaction partners. *iScience* 2022;25:103808.
- 45 Boeynaems S, Alberti S, Fawzi NL, et al. Protein phase separation: a new phase in cell biology. *Trends Cell Biol* 2018;28:420–35.
- 46 Yoshizawa T, Nozawa R-S, Jia TZ, et al. Biological phase separation: cell biology meets biophysics. *Biophys Rev* 2020;12:519–39.
- 47 Schlenk RF, Döhner K, Kneba M, et al. Gene mutations and response to treatment with all-trans retinoic acid in elderly patients with acute myeloid leukemia. results from the amlsg trial AML hd98b. *Haematologica* 2009;94:54–60.
- 48 Burnett AK, Hills RK, Green C, et al. The impact on outcome of the addition of all-trans retinoic acid to intensive chemotherapy in younger patients with nonacute promyelocytic acute myeloid leukemia: overall results and results in genotypic subgroups defined by mutations in NPM1, FLT3, and CEBPA. *Blood* 2010;115:948–56.
- 49 Drach J, McQueen T, Engel H, et al. Retinoic acid-induced expression of CD38 antigen in myeloid cells is mediated through retinoic acid receptor-alpha. *Cancer Res* 1994;54:1746–52.